Energetics and Structure of the 1- and 2-Adamantyl Radicals and Their Corresponding Carbonium Ions by Photoelectron Spectroscopy

Gary H. Kruppa and J. L. Beauchamp*

Contributon No. 7190 from the Arthur Amos Noyes Laboratory of Chemical Physics, California Institute of Technology, Pasadena, California 91125. *Received October 28, 1985*

Abstract: The first photoelectron bands of the 1- and 2-adamantyl radicals, formed by flash vacuum photolysis of 1- and 2-adamantylmethyl nitrite, have been obtained. The adiabatic (IP_a) and vertical (IP_v) ionization potentials of the 1-adamantyl radical are 6.21 ± 0.03 and 6.36 ± 0.05 eV, respectively. IP_a and IP_v for the 2-adamantyl radical are 6.73 ± 0.03 and 6.99 ± 0.05 eV, respectively. The difference in hydride affinities between the 1-adamantyl and *tert*-butyl cations (Sharma, R. B.; Sen Sharma, D. K.; Hiraoka, K.; Kebarle, P. *J. Am. Chem. Soc.* **1985**, *107*, 3747) combined with the difference in IP_a between the *tert*-butyl and 1-adamantyl radicals (0.49 ± 0.06 eV) yield a value of 99 kcal/mol for the tertiary C–H bond energy in adamantane, 3.7 ± 1.2 kcal/mol greater than the tertiary C–H bond energy in isobutane (assumed to be 95 kcal/mol). The effects of the geometrical constraints imposed by the adamantyl cage on the homolytic and heterolytic C–H bond cleavage energies are discussed for the 1- and 2-adamantyl cases. The width of the Franck–Condon envelope obtained is related to the geometry changes that occur upon ionization. The surprisingly broad envelope observed for the **planar** 2-adamantyl radical indicates that the Franck–Condon envelope for the 1-admantyl radical should not be interpreted as exclusively due to changes at the bridgehead position. Thermal decomposition products of the 1- and 2-adamantyl radicals are observed, and the pathways for thermal decompositions of the radicals are discussed. To confirm expected trends in ionization potentials and band shapes of tertiary radicals, the first photoelectron band of the 2-methyl-2-butyl radical has been obtained. The IP_a of the 2-metyl-2-butyl radical is 6.65 ± 0.04 eV with IP_v = 6.91 ± 0.05 eV.

Compared to acyclic hydrocarbons, the unique geometry of adamantane imposes constraints on the energetics of forming four of the possible reactive intermediates (I–IV) that can be generated by homolytic and heterolytic carbon–hydrogen bond cleavage.[1]

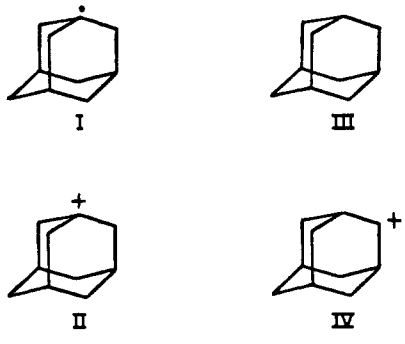

I III II IV

Starting from the tetrahedral configuration, the reactive centers in I–IV will relax in the direction of a planar configuration, subject to the geometric constraints imposed by the adamantyl cage. The effects of the constrained geometry on the rates of reactions that are believed to involve species I–IV as intermediates are of particular interest.[2] The thermodynamic stablities of I and II relative to the *tert*-butyl radical and cation are also of interest since II has been predicted to be unusually stable in the gas phase.[3]

As the reactive centers in I–IV attempt to adopt the preferred configuration, the strain energy increases as a result of distortion in the rigid tetrahedral ring system to accomodate the planar center. The change in strain energy on going from the parent hydrocarbon to the reactive intermediate will be referred to as Δ (strain energy). Studies of the thermal decomposition rates of azoalkanes,[4] peresters,[5] and rates of other reactions that are believed to reflect radical stabilities[6] indicate that the Δ(strain energy) for the formation of I from adamantane is substantially greater than the Δ(strain energy) for the formation of *tert*-butyl radicals. Recent thermolysis studies of compounds V[7] and VI[8]

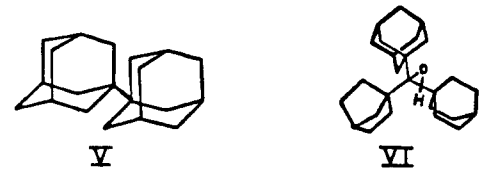

V VI

have been interpreted as showing that the formation of I has a greater Δ(strain energy) than *tert*-butyl radical by 0 and 2.2 kcal/mol, respectively. An empirical-force field calculation has yielded a value of 1.4 kcal/mol for this difference.[8] These studies provide qualitative estimates of the Δ(strain energy) for the formation of I that cover a range of values that may in part be due to phenomena such as polar and steric effects,[9] rather than incipient radical stability, that may influence reaction rates.

Information on the geometry of I is available from ESR experiments,[10] which indicate that the bridgehead radical site is only slightly flattened from tetrahedral geometry. An ESR study of the 2-adamantyl radical indicates that the radical site in III is planar.[11]

There have been a number of previous gas-phase studies of the stability, geometry, and Δ(strain energy) of II. The gas-phase

(1) (a) Fort, R. C.; Schleyer, P. v. R. *Adv. Alicyclic Chem.* **1966**, *1*, 283. (b) Ruchardt, C. *Angew. Chem., Int. Ed. Engl.* **1970**, *9*, 830.
(2) (a) Engel, P. S. *Chem. Rev.* **1980**, *80*, 99. (b) Bingham, R. C.; Schleyer, P. v. R. *Tetrahedron Lett.* **1971**, 23.
(3) (a) Houriet, R.; Schwarz, H. *Angew. Chem., Int. Ed. Engl.* **1979**, *18*, 951. (b) Staley, R. H.; Wieting, R. D.; Beauchamp, J. L. *J. Am. Chem. Soc.* **1977**, *99*, 5964.
(4) Golzke, V.; Groeger, F.; Boerlinner, A.; Ruchardt, C. *Nouv. J. Chim.* **1978**, *2*, 169.
(5) Fort, R. C.; Franklin, R. E. *J. Am. Chem. Soc.* **1968**, *90*, 5267. Lorand, J. P.; Chodroff, S. D.; Wallace, R. w. *Ibid.* **1968**, *90*, 5266. Humphrey, C. B.; Hodgson, B.; Pincock, R. E. *Can. J. Chem.* **1968**, 3099.
(6) See ref 2a for a summary of experiments completed before mid-1979.
(7) Beckhaus, H. D.; Flamm, M. A.; Ruchardt, C. *Tetrahedron Lett.* **1982**, *23*, 1805.
(8) Lomas, S. J.; Dubois, J. E. *Tetrahedron Lett.* **1983**, *24*, 1161.
(9) See ref 1b, 2a, and references contained therein for a more complete discussion of factors, other than incipient radical stabilities, that can influence pyrolysis rates.
(10) (a) Krusic, P. J.; Rettig, R. A.; Schleyer, P. v. R. *J. Am. Chem. Soc.* **1972**, *94*, 995. (b) Mishra, S. P.; Symons, M. C. . *Tetrahedron Lett.* **1983**, *25*, 2267.
(11) Kira, M.; Watanabe, M.; Ichinose, M.; Sakurai, H. *J. Am. Chem. Soc.* **1982**, *104*, 3762.

0002-7863/86/1508-2162$01.50/0

Table I. Gas-Phase Studies Relating to Ion Stability

reaction[a]	$\Delta G°$, kcal/mol	$\Delta H°$,[b] kcal/mol	$\Delta S°$, eu
$t\text{-}C_4H_9^+ + C_{10}H_{16} \rightarrow i\text{-}C_4H_{10} + C_{10}H_{15}^+$	−8.24	−7.62 ± 0.1	−2.06
$t\text{-}C_4H_9^+ + C_{10}H_{15}Cl \rightarrow i\text{-}C_4H_{10}Cl + C_{10}H_{15}^+$[c]		−6.3 ± 0.1	
$t\text{-}C_4H_9^+ + C_{10}H_{15}Br \rightarrow i\text{-}C_4H_{10}Br + C_{10}H_{15}^+$[d]		−10.8 ± 10	
$t\text{-}C_4H_9^+ + C_{10}H_{15}Br \rightarrow i\text{-}C_4H_{10}Br + C_{10}H_{15}^+$[e]		≤4.0	
$t\text{-}C_4H_9^+ + C_{10}H_{16} \rightarrow i\text{-}C_4H_{10} + C_{10}H_{15}^+$[f]		−4.1	
$t\text{-}C_4H_9^+ + i\text{-}C_5H_{12} \rightarrow i\text{-}C_4H_{10} + t\text{-}C_5H_{11}^+$[g]	−2.5	−3.3 ± 0.2	−2.7

[a] $C_{10}H_{16}$ refers to adamantane, $C_{10}H_{15}X$ (X = Cl and Br) refers to the 1-halo-adamantane, and $C_{10}H_{15}^+$ is assumed to be the 1-adamantyl ion. [b] $\Delta H°$ in this column yields the differences in hydride or halide affinities of the carbonium ions. [c] High-pressure mass spectrometry results, ref 12. [d] ICR equilibrium study, ref 3b. [e] ICR equilibrium study, ref 3a. [f] Calculated, ref 13. [g] High-pressure mass spectrometry, ref 34.

stability of II relative to $(CH_3)_3C^+$ has been determined by equilibrium studies using high-pressure mass spectrometry. For reaction 1, these measurements yielded $\Delta H° = -7.62 \pm 0.1$

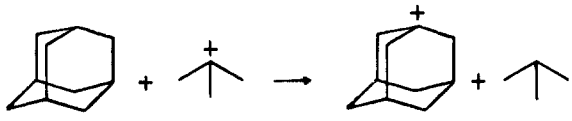

(1)

kcal/mol and $\Delta S° = 2.1$ eu.[12] This result is in good agreement with previous gas-phase equilibrium results from ICR mass spectrometry[3b] and calculations,[13] which are summarized in Table I. Theoretical calculations have shown that there is a substantial difference in geometry between the minimum energy structure for adamantane and the minimum energy structure for II.[13] The formation of II from adamantane has been shown to have a Δ(strain energy) of 12 kcal/mol by an empirical force field (EFF) calculation.[14]

Photoelectron spectroscopy (PES) of free radicals offers an opportunity to interrelate directly the structure and energetics of a radical and its corresponding carbonium ion. In the general ionization process 2 the spectrum of electron kinetic energies

$$R\cdot + h\nu \rightarrow R^+ + e^- \qquad (2)$$

corresponding to ionization to the ground electronic state of R^+ contains information about the changes in geometry and force constants that occur in forming R^+ from R·. Since the ionization potentials of radicals are lower than those of stable species, the first band of the radical spectrum is at higher electron kinetic energies than the first band of stable species. Low concentrations of radicals (~0.1–0.01%) can easily be detected because the background signal in the high kinetic energy region is small. For systems with minor geometry differences between R· and R^+ (e.g., methyl,[15] allyl,[16] and benzyl[16]) the first band of the photoelectron spectrum is sharp with $IP_a = IP_v$. For other systems, where there is a large difference in geometry between R· and R^+, a broad Franck–Condon envelope for the first photoelectron band is observed, with a large difference between IP_a and IP_v (e.g., *tert*-butyl, where $IP_v - IP_a = 0.22$ eV[17]). In the present work, an investigation of the first photoelectron bands of I and III is presented. In these cases the rigid adamantyl ring system introduces a substantial increase in strain energy when the radicals or ion centers attempt to achieve a planar configuration.[14] The constraints of the ring system should be reflected in the observed Franck–Condon envelopes and the differences between IP_a and IP_v for I and III. Useful thermochemical information can also be derived from the photoelectron spectrum. The difference in

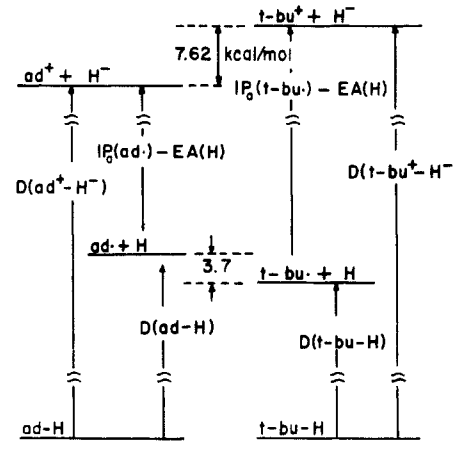

Figure 1. Thermochemical cycle showing the quantities relating the relative hydride affinities and relative homolytic bond dissociation energies for the tertiary bonds in adamantane and isobutane.

IP_a between I and *tert*-butyl radical can be used with the difference in hydride affinities between II and $(CH_3)_3C^+$ to obtain the difference in tertiary C–H bond energies (see Figure 1 for the factors relating these quantities). The differences in bond energies can be used to discuss the changes in strain energies for the formation of I and *tert*-butyl radical without some of the effects that may complicate the interpretation of the pyrolysis experiments mentioned above.

Only one other tertiary hydrocarbon radical, the *tert*-butyl radical, has previously been studied by PES.[15c,17] To confirm expected trends in ionization potentials and band shapes, the first photoelectron band of the 2-methyl-2-butyl radical has been obtained in this work.

Photoelectron bands that correspond to thermal decomposition products of the 1- and 2-adamantyl radicals are observed in this work, and the pathway for thermal decomposition of the two radicals are discussed.

Experimental Section

The apparatus used in these experiments is a photoelectron spectrometer specifically designed to study the products of pyrolysis reactions. It has been described in detail elsewhere.[16]

The radicals studied in this work were produced by the pyrolysis of the appropriate alkyl nitrites, reactions 3 and 4. The pyrolyzer used in

$$RCH_2ONO \rightarrow RCH_2O + NO \qquad (3)$$

$$RCH_2O \rightarrow R + CH_2O \qquad (4)$$

this study was 2 cm in length, corresponding to the "long" pyrolyzer used in an earlier study.[18] 2,2-Dimethyl-1-butyl nitrite was prepared from 2,2-dimethyl-1-butanol, obtained from Overlook Industries, Inc., by a standard method.[19] 1-Adamantylmethyl nitrite was prepared from 1-adamantanemethanol, obtained from Aldrich, using the same standard method with slight modifications. $NaNO_2$ (2.3 g, 33.3 mmol) and 1-adamantanemethanol (5.00 g, 32.1 mmol) were dissolved in 100 mL of 20% aqueous THF. This was stirred in an ice bath, and 16 mL of 2 M

(12) Sharma, R. B.; Sen Sharma, D. K.; Hiraoka, K.; Kebarle, P. *J. Am. Chem. Soc.* **1985**, *10m*, 3747.
(13) Sunko, D. E.; Hirsl-Starcevic, S.; Pollack, S. K.; Hehre, W. J. *J. Am. Chem. Soc.* **1979**, *101*, 6163.
(14) Bingham, R. C.; Schleyer, P. v. R. *J. Am. Chem. Soc.* **1971**, *93*, 3189.
(15) (a) Dyke, J.; Jonathan, N.; Lee, E.; Morris, A. *J. Chem. Soc., Faraday Trans. 2* **1976**, *72*, 1385. (b) Koenig, T.; Balle, T.; Snell, W. *J. Am. Chem. Soc.* **1975**, *97*, 662. (c) Koenig, T.; Balle, T.; Chang, J. C. *Spectrosc. Lett.* **1976**, *9*, 755.
(16) Houle, F. A.; Beauchamp, J. L. *J. Am. Chem. Soc.* **1978**, *100*, 3290.
(17) (a) Houle, F. A.; Beauchamp, J. L. *J. Am. Chem. Soc.* **1979**, *101*, 4067. (b) Dyke, J.; Jonathan, N.; Lee, E.; Morris, A.; Winter, M. *Phys. Soc.* **1977**, *16*, 197.
(18) Schultz, J. C.; Houle, F. A.; Beauchamp, J. L. *J. Am. Chem. Soc.* **1984**, *106*, 3917.
(19) Levin, N.; Hartung, W. *Organic Syntheses*; Wiley: New York, 1955; Collect. Vol. III, p 192.

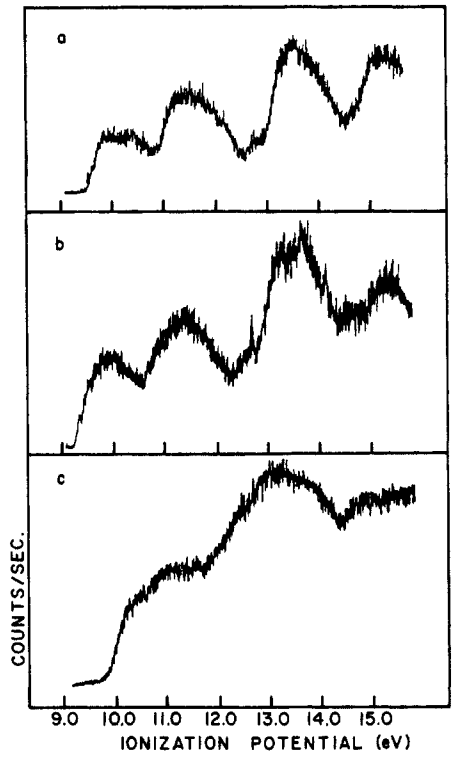

Figure 2. Room temperature photoelectron spectra of the nitrite precursors to the radicals used in this study: (a) 1-adamantylmethyl nitrite; (b) 2-adamantylmethyl nitrite; (c) 2,2-dimethyl-1-butyl nitrite.

H_2SO_4 was added over 1 h. The solution was stirred for 1 h and warmed to room temperature. $CHCl_3$ (10 mL) was added, the organic layer was separated, and the volume was reduced on a rotary evaporator. The purity of the clear yellow liquid obtained in approximately 80% yield was checked by NMR spectroscopy. 2-adamantylmethyl nitrite was prepared from 2-adamantanone obtained from Aldrich. The 2-adamantanone was first converted to 2-methyleneadamantane via a Wittig reaction[20] followed by hydroboration to obtain 2-adamantanemethanol.[21] The 2-adamantanemethanol obtained (in about 50% yield from the 2-adamantanone) was converted to 2-adamantylmethyl nitrite by the method for 1-adamantylmethyl nitrite described above. For the 2-adamantanemethanol case, the conversion to nitrite went only 50% to completion, but it was found to be unnecessary to separate the alcohol and nitrite since the alcohol had insufficient vapor pressure at room temperature to interfere with the spectrum of the nitrite.

The pyrolysis spectra were obtained with both HeI and NeI radiation. The band shapes obtained with the HeI and NeI radiation sources were the same within experimental error. The pyrolysis spectra were obtained at temperatures from 350 to 500 °C. The energy scale was calibrated with the He Iα and He Iβ bands of CH_3I, CH_2O, Xe, and Ar. The resolution for these experiments is 30–40 mV as determined from the full width at half-maximum of Ar $^2P_{3/2}$ band. 1-1′-azoadamantane was also tried as a source of 1-adamantyl radicals, but a sufficient vapor pressure of the azo compound could not be obtained in the pyrolyzer due to the sample handling system, which cannot be uniformly heated.

Results

The HeI photoelectron spectrum of the nitrite precursors to I are shown in Figure 2. The adiabatic IP's of the first bands are 9.56, 9.25, and 9.92 eV for 1-adamantylmethyl nitrite, 2-adamantylmethyl nitrite, and 2,2-dimethyl-1-butyl nitrite, respectively, where the errors are ±0.05 eV and the energy scale was calibrated with the He Iα bands of Ar. Spectra from 5.9 to 7.5 eV of the pyrolysis products of the 1-adamantylmethyl nitrite are shown in Figure 3. Figure 3a shows the spectrum at 355 °C, where about 25% of the precursor decomposes (the amount of decomposition is estimated from the relative intensities of the pyrolysis product bands, the CH_2O band, and the nitrite bands). Figure 3bv shows the spectrum at 430 °C, where 50% of the

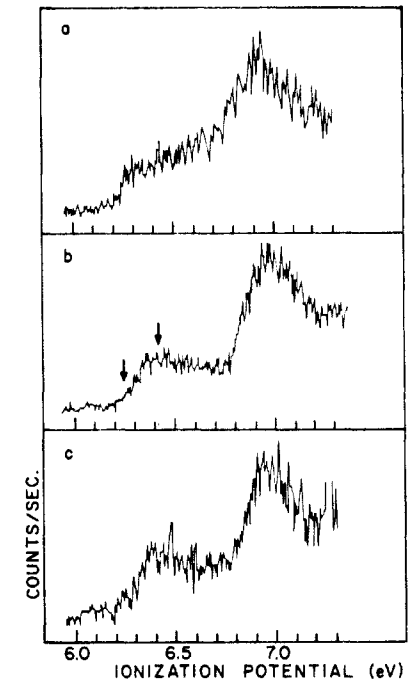

Figure 3. Photoelectron spectra of the pyrolysis product of 1-adamantylmethyl nitrite (1-adamantyl radical) in the energy range 6.0–7.4 eV at (a) 355 °C; (b) 430 °C; (c) 470 °C. Estimated adiabatic and vertical ionization potentials are indicated by arrows in (b).

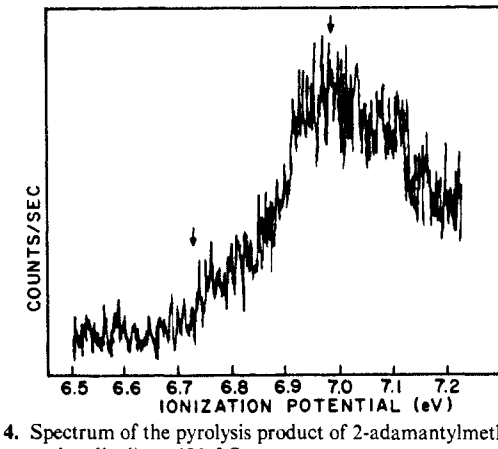

Figure 4. Spectrum of the pyrolysis product of 2-adamantylmethyl nitrite (2-adamantyl radical) at 480 °C.

precursor decomposes. Finally, Figure 3c shows the spectrum at 470 °C, where pyrolysis is 60–80% complete. The observed band shapes were reproduced at a given temperature over several days. Over longer periods of time the quartz pyrolyzer surface became coated with carbon deposits, and the temperature at which a particular band shape was observed shifted to lower temperature. A spectrum of the pyrolysis products of 2-adamantylmethyl nitrite at 480 °C is shown in Figure 4. The spectrum of the pyrolysis products of 2,2-dimethyl-1-butyl nitrite from ~6.5 to 7.4 eV is shown in Figure 5. The observed band shapes did not change with temperature.

The first point to be made about the photoelectron bands presented in Figure 3 is that the bands are due to He Iα ionization of alkyl radicals, produced by pyrolysis, and not He Iβ or He Iγ ionization of the nitrite precursor. Since the first adiabatic IP of the precursor is at about 9.45 eV (see Figure 2), a weak band due to ionization of the nitrite by He Iγ radiation (which is <1% of the total intensity of the He UV lamp output) would appear about 7.0 eV. Bands due to He Iβ ionization (which is a stronger impurity line, about 2% of the total HeI lamp output) would not appear below 7.58 eV. This is confirmed by room temperature spectra of the region 5.9–8.0 eV, taken with collection times similar to those used to produce the spectra in Figures 3, which show no

(20) Wittig, G.; Schoelkopf, U. *Org. Syn.* **1960**, *40*, 66.
(21) Brown, H. C. *Organic Syntheses via Boranes*; Wiley: New York, 1975; pp 23–24.

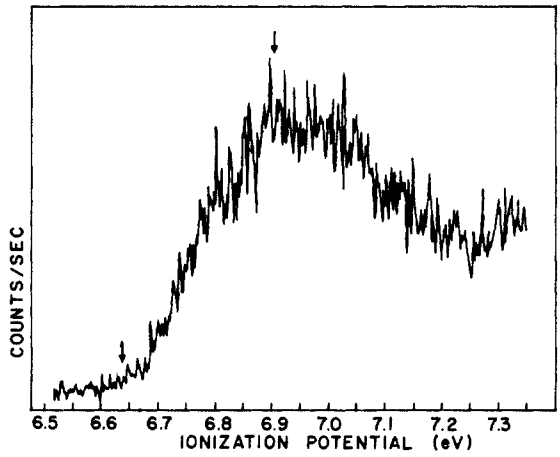

Figure 5. Spectrum of the pyrolysis product of 2,2-dimethyl-1-butyl nitrite (2-methyl-2-butyl radical) at 400 °C.

peaks below 7.0 eV. In addition, a spectrum was taken of the pyrolysis products at 430 °C using NeI radiation, and the band shape observed was close to that in Figure 3b.

Discussion

Identification of Radicals. An important feature of the spectra in Figure 3 is the change in band shapes and relative intensities with temperature, especially in going from 355 to 430 °C. The IP_a of the first band remains constant with temperature and was determined to be 6.21 ± 0.03 eV. No low-lying excited electronic states are expected in the 1-adamantylcarbonium ion. Hence the data in Figure 3 indicate the presence of at least two radicals and possibly a third. The additional radicals result from the thermal decomposition of 1-adamantyl radicals prior to ionization. Lossing[22] has previously noted this difficulty in attempts to measure the ionization potentials of the 1- and 2-norbornyl and 1-bicyclo[2.2.2]octyl radicals formed by pyrolysis of the corresponding alkyl nitrites, using monoenergetic electron impact ionization and mass spectrometry detection. Only rearrangement products of the desired norbornyl and bicyclooctyl radicals were observed in the mass spectrometer. An RRKM calculation was performed in order to determine the feasibility of observing adamantyl radicals as the product of reactions 3 and 4 in the photoelectron spectrometer. Typical activation energies for reactions 3 and 4 are 37 and 12 kcal/mol, respectively,[23] and the residence time in the pyrolyzer is about 1 ms. A reasonable value of the activation energy for subsequent decomposition of the 1-adamantyl radical is 25 kcal/mol.[24] The RRKM calculation shows that even under conditions where the rate constants for the reactions 3 and 4 are large enough so that most of the nitrite decomposes to adamantyl radicals, the resulting adamantyl radicals have internal energies of ~10 kcal/mol. This is well below the 25 kcal/mol required for decomposition or rearrangement. Hence, any decomposition or rearrangement products observed are the result of adamantyl radicals undergoing further energizing collisions with the hot pyrolyzer wall after they have been produced from the nitrite. Since residence times in the pyrolyzer are short, some of the adamantyl radicals should escape from the pyrolyzer to be detected.

Ionization potentials of alkyl radicals generally decrease in the order primary > secondary > tertiary. There is also a qualitative correlation between ionization potentials and the number of carbons in a primary, secondary, or tertiary radical as shown in Figure 6.[25] Based on these correlations, the band in Figure 3 with the adiabatic IP of 6.21 ± 0.03 eV can be confidently assigned to ionization of I. Inspection of Figure 6 and general trends in ionization potentials of alkyl radicals show that only a large tertiary radical such as I would be expected to have an IP as low as 6.21 eV. From inspection of a number of spectra with the best signal-to-noise ratios, IP_v(I) is estimated to be 6.36 ± 0.05 eV. The second band in Figure 3 in the region 6.5–7.0 eV is probably due to thermal decomposition products of I and will be discussed further below.

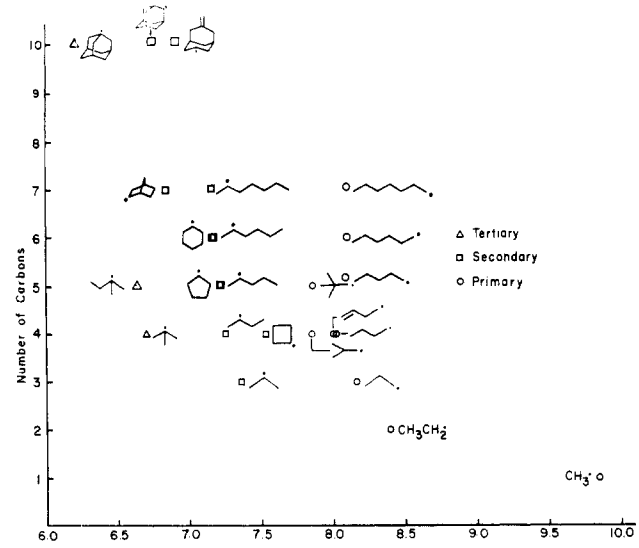

Figure 6. Correlation of the IP_a of primary, secondary, and tertiary alkyl radicals with the number of carbon atoms. Ionization potentials are from ref 25.

The band shown in Figure 4 is assigned to ionization of the 2-adamantyl radical. The IP_a of 6.73 eV for this radical fits well on Figure 6. The IP_v is 6.99 ± 0.05 eV.

The band in Figure 5 is assigned to ionization of the 2-methyl-2-butyl radical. The IP_a of the 2-methyl-2-butyl radical obtained in this work is 6.64 ± 0.04 eV and the IP_v is 6.91 ± 0.05 eV. This value is in reasonable agreement with an earlier determination by nitrite pyrolysis followed by monoenergetic electron impact ionization, which gave a value of 6.85 eV for IP_a of the 2-methyl-2-butyl radical.[26] Also, the IP_a determined in this work for the 2,2-dimethyl-1-butyl radical fits well on Figure 6.

Thermal Decomposition of 1- and 2-Adamantyl Radicals. Previous studies have shown that photoelectron spectroscopy is a useful tool for elucidating the thermal decomposition pathways of alkyl radicals,[27] and in this section a discussion of the thermal decomposition pathways of the 1- and 2-adamantyl radicals is presented. Alkyl radicals may decompose by β-CC and β-CH cleavages as well as more complex skeletal rearrangements.[28] The thermal decomposition of 1-adamantyl radicals has been studied by gas chromatographic analysis of the products of pyrolysis of 1-nitroadamantane.[29] Orbital overlap considerations suggest that

(22) McAllister, J.; Dolesek, Z.; Lossing, F. P.; Gleiter, B.; Schleyer, P. v. R. *J. Am. Chem. Soc.* **1967**, *89*, 5982.

(23) Benson, S. W. *Thermochemical Kinetics*; Wiley: New York, 1968; pp 464 ff.

(24) Reference 23, pp 567 ff. No direct experimental data are available on the activation energy for the decomposition of I, but this reference contains data for other simple alkyl radicals. The value of 25 kcal/mol was chosen because it is at the lower end of the range of values observed for other radicals, which might be expected for I since the orbitals are favorably oriented for decomposition. See also the discussion in ref 22.

(25) The ionization potentials plotted in Figure 6 are from this work and the following references: (a) ref 16; (b) ref 17a; (c) ref 18; (d) Schultz, J. C.; Houle, F. A.; Beauchamp, J. L. *J. Am. Chem. Soc.* **1984**, *106*, 7336; (e) Houle, F. A. Ph.D. Thesis, California Institute of Technology, Pasadena, CA, 1979. (f) Dearden, D. V.; Beauchamp, J. L. *J. Am. Chem. Soc.* **1985**, *89*, 5359.

(26) Lossing, F. P.; Maccoll, A. *Can. J. Chem.* **1976**, *54*, 990. Lossing also obtained a higher value for the IP_a of the *tert*-butyl radical than the value from this laboratory (ref 17). The difference between 2-methyl-2-butyl radical and the *tert*-butyl radical IP_a from PES measurements is 0.06 eV, which is close to the difference obtained by Lossing, 0.08 eV. Hence, it appears that Lossing's measurements do not measure the true adiabatic IP of alkyl radicals. Interestingly, the IP's obtained by Lossing are close to the vertical IP's measured by PES.

(27) Houle, F. A.; Beauchamp, J. L. *J. Phys. Chem.* **1981**, *85*, 3456.

(28) Pryor, W. A. *Free Radicals*; Wiley-Interscience: New York, 1973; Vol. 1. Kossiakoff, A.; Rice, F. O. *J. Am. Chem. Soc.* **1943**, *65*, 590.

(29) Fields, E. K.; Meyerson, S. *Adv. Free Radical Chem.* **1975**, *5*, 178.

Scheme I

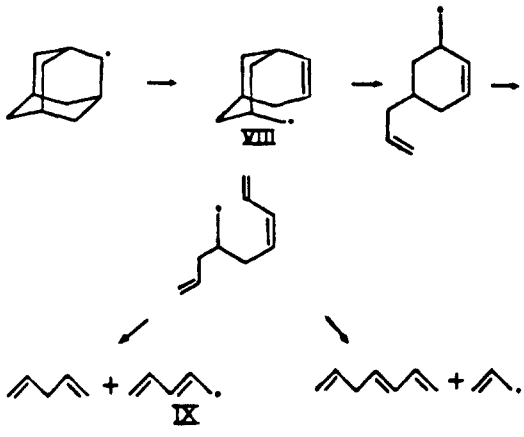

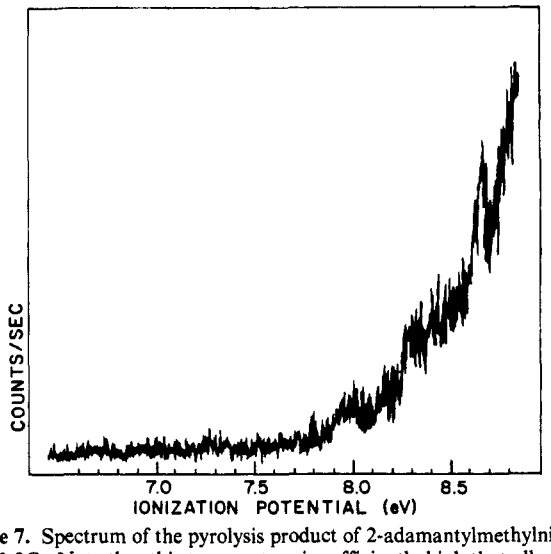

Figure 7. Spectrum of the pyrolysis product of 2-adamantylmethylnitrite at 550 °C. Note that this temperature is sufficiently high that all of the 2-adamantyl radical decomposes before entering the source chamber of the photoelectron spectrometer.

the 1-adamantyl radical would most likely undergo β-CC cleavage to yield the radical VII. Inspection of the trends in Figure 6 shows

that a large secondary radical such as VII would be expected to have an IP_a in the range 6.5–7.0 eV. This possibility is confirmed by the spectrum of 2-adamantyl radical in Figure 4 with an IP_a of 6.73 eV, which shows that a large secondary radical such as VII could have an IP_a low enough to be responsible for the second band in Figure 3. Further decomposition of radical VII by successive β-CC or β-CH cleavages leads to a series of secondary radicals and stable alkenes. The topology of the 1-adamantyl radical is such that it can open to a series of secondary radicals but it can never come apart to give primary radicals by β-CC cleavage.

The 2-adamantyl radical can open to a series of primary radicals by β-CC cleavage and can cleave to smaller radicals (see Scheme I). The initial radicals resemble isobutyl radical in that the radical site is α to a tertiary carbon. Figure 7 shows the pyrolysis products of 2-adamantylmethyl nitrite at 550 °C, a temperature sufficiently high that all of the 2-adamantyl radical produced decomposes before being detected. Although it is not very distinctive, the band at 7.84 eV in Figure 7 has an IP_a just below that of isobutyl (IP_a = 7.93 eV[25d]) and may be due to radical VIII. Further decomposition of the radical VIII by successive β-cleavages, Scheme I, leads to a series of primary radicals and finally the allyl radical

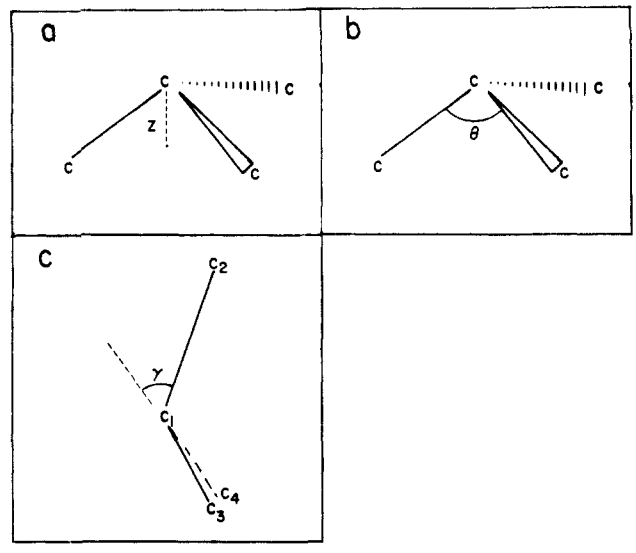

Figure 8. Three commonly used measures of nonplanarity at a carbon center: (a) out-of-plane distance, z; (b) C–C–C bond angle θ; (c) out-of-plane angle, γ. These parameters are discussed further in the text.

Table II. Comparison of Out-of-Plane Angles γ[a] for the *tert*-Butyl and 1-Adamantyl Radicals and Ions

	adamantyl	*tert*-butyl
γ (radical)	43.4°[b]	22.1°[e]
γ (ion)	29.6°[c]	0°
difference	13.8°	22.1°
$IP_v - IP_a$	0.15 eV[d]	0.22 eV[g]

[a] See text for the definition of γ. [b] Reference 10. [c] Reference 13. [d] This work. [e] Reference 31. [f] The difference between the vertical and adiabatic IP's of the radical. [g] Reference 17a.

and radical IX. There is no obvious evidence for the allyl radical (IP_a = 8.17 eV) or IX ($IP_a \simeq$ 7.25 eV)[30] in Figure 7, but the decomposition pathway is complicated by the possibility of intramolecular hydrogen abstractions in the intermediates leading to these species.[28] The complexities arising from the possibility of hydrogen abstractions and β-CH cleavages make it difficult to assign all of the products in the region 8.1–9.0 eV in Figure 7. While PES cannot be used to identify all of the products of hydrocarbon pyrolysis, it is a unique method that can be used to directly observe the reactive intermediates that can only be inferred in mechanisms derived from gas chromatographic product studies. For this reason, PES studies of hydrocarbon pyrolysis are a useful complement to GC product studies.[18,25b,25d,27]

Geometries of the Carbonium Ions and Radicals. Several measures of nonplanarity at a radical or ion center have been used previously in the literature, and these are illustrated in Figure 8. Figure 8a shows the distance z, defined as the perpendicular distance from the spin-bearing or positive carbon to the plane containing the three α carbons. The angle θ is defined simply as the C–C–C bond angle (Figure 8b). Figure 8c shows the angle γ, which is defined as the angle between the bond formed by C_1 and C_2 and the plane formed by C_1 and the remaining carbons, C_3 and C_4. ESR data for I indicate that the distance z is 0.4 Å, a flattening of only 0.1 Å from tetrahedral geometry.[10] Yoshimine and Pacansky[31] have performed ab initio SCF calculations to determine the optimum geometries of isobutane and the *tert*-butyl radical. The calculations show that the angle γ (Figure 8c) is 22.1° for the *tert*-butyl radical. Hehre[13] and co-workers have calculated the optimum geometry for II and found the C–C bonds α to the carbocation center shortened by 0.043 Å from the length in adamantane, β–γ C–C bonds lengthened by 0.050 Å, and the C–C–C bond angle at the carbocation center opened to 117.5°. The *tert*-butyl cation is known to be planar. These geometrical

(30) Lossing, F. P.; Holmes, J. *Int. J. Mass Spectrom. Ion Phys.* **1976**, *19*, 9.

(31) Yoshimine, M.; Pacansky, J. *J. Chem. Phys.* **1981**, *74*, 5168.

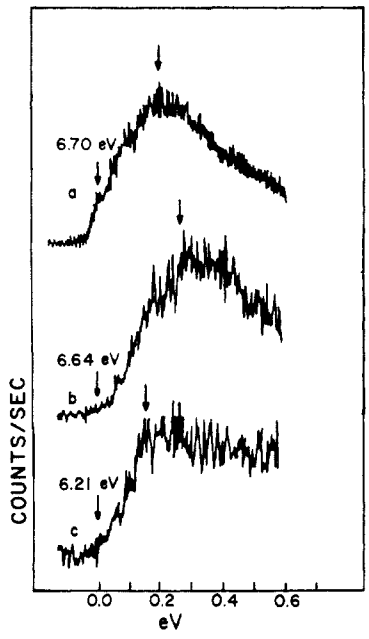

Figure 9. Photoelectron spectra of the three tertiary radicals that have been studied to date: (a) *tert*-butyl radical (from ref 17a); (b) 2-methyl-2-butyl radical from this work; (c) 1-adamantyl radical from this work. The spectra are shown so that the adiabatic ionization potentials coincide on the x axis, and the scale is in electron volts above the adiabatic ionization potential.

results are summarized in Table II, where they have all been converted to the out-of-plane angle γ for purposes of comparison. The substantial geometry difference between I and II predicted by the ESR data and the calculation is supported by the broad Franck–Condon envelope for the first photoelectron band of I with a 0.15-eV difference between IP_a and IP_v observed in this study. Table II also shows that the difference between IP_a and IP_v correlates well with the differences in geometries between the radical and cation. Figure 9 shows the photoelectron spectra of the two tertiary radicals measured in this study along with the spectrum of the *tert*-butyl radical. Interference in the 1-adamantyl radical spectrum from the spectrum of thermal decomposition products makes it difficult to compare the band for 1-adamantyl radical to the others in Figure 9. However, it is clear that the 1-adamantyl radical has a sharper onset and greater slope in the rising portion of the band than *tert*-butyl radical. The geometry changes that occur upon ionization of the 2-methyl-2-butyl radical are not known quantitatively, but the added methylene group would be expected to allow a greater geometrical change to stabilize the ion than is seen for the *tert*-butyl radical. As can be seen from Figure 9, 2-methyl-2-butyl radical has the broadest photoelectron band, with the least slope in the rising portion of the band. Hence the band widths, the difference between IP_a and IP_v, and the slopes in the rising portions of the bands all correlate well with the extent of geometrical reorganization expected upon ionization of these radicals.

The 2-adamantyl radical has been studied previously by ESR,[11] and the ESR data indicate that the radical center is planar. Since carbonium ions are also known to prefer planarity, a sharp first photoelectron band might be expected for the 2-adamantyl radical, as is the case for methyl radical, where both the cation and radical are known to be planar.[15] In Figure 10 the first band of 2-adamantyl radical is plotted on the same scale as 2-propyl radical for comparison. Figure 10 shows that the first band of 2-adamantyl is sharper than a typical secondary radical, but it is not as sharp as would be expected for a planar alkyl radical (e.g., methyl, allyl). Either the 2-adamantyl radical is not planar or the possibility of other factors leading to a broad Franck–Condon envelope must be considered. One such factor is that while the radical may be planar, as the ESR data indicate, it is unlikely that the C–C–C bond angle at the radical center is 120° due to the constraints of the adamantyl cage. This bond angle in the

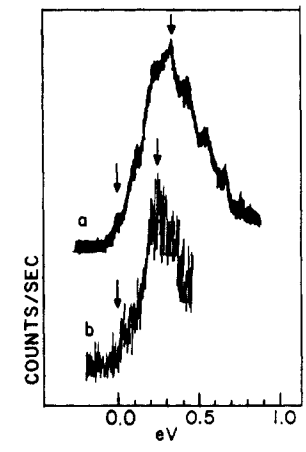

Figure 10. Photoelectron spectra of (a) 2-propyl radical (from ref 17a), and (b) 2-adamantyl radical. The spectra are plotted so that the adiabatic ionization potentials coincide on the x axis, and the scale is in electron volts above the adiabatic ionization potential.

parent hydrocarbon is 108.8° ± 1°.[32] For comparison (from Table II), the C–C–C angle in I is 112° at the bridgehead position. Carbonium ions strongly prefer a planar sp^2 geometry with C–C–C bond angles of 120°, so that the width of the 2-adamantyl band may be due to the bond angles in the radical distorting toward 120° upon ionization. Structural relaxation at the sites β and γ to the ion center, which is known to occur in the formation of the 1-adamantyl cation,[13] may also be contributing to the width of the Franck–Condon envelope.

Radical and Ion Thermochemistry. From the data for the hydride transfer reaction 1 and the difference in IP_a between I and *tert*-butyl radical,[17] adamantane is found to have a tertiary C–H bond dissociation energy 3.7 ± 1.2 kcal/mol greater than isobutane (see Figure 1 for the factor relating these quantities). The absolute value for the tertiary C–H bond dissociation energy in adamantane is 98.5 ± 1.5 kcal/mol, assuming a tertiary bond dissociation energy of 95 ± 1 kcal/mol in isobutane. The thermochemical data used in these calculations and the errors associated with them are discussed in the Appendix. In a condensed-phase study, 1-adamantyl radicals were found to abstract hydrogen from solvents such as cyclohexane,[33] implying that the tertiary C–H bond in adamantane is stronger than a typical secondary C–H bond and supporting the high tertiary bond energy found for adamantane in this study.

Similar data can be derived for the 2-methyl-2-butyl radical using the reported value of $\Delta H°$ for reaction 5 (−3.37 ± 0.20

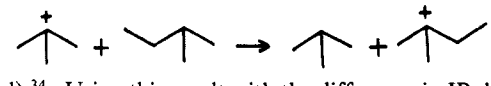
(5)

kcal/mol).[34] Using this result with the difference in IP_a between *tert*-butyl[15] and 2-methyl-2-butyl radicals (0.06 eV) gives a tertiary bond energy for isopentane 2.0 ± 1.7 kcal/mol lower than the tertiary bond energy in isobutane. As expected, the added methylene has a slightly stabilizing effect in the radical and a greater stabilizing effect in the 2-methyl-2-butyl cation.

No data on the relative hydride affinity of the 2-adamantyl cation are available from high-pressure mass spectrometry equilibrium studies or other techniques. Assuming a typical secondary C–H bond dissociation energy of 96 kcal/mol in adamantane gives a heat of formation for the 2-adamantyl radical of 12.3 kcal/mol. Combining this with the IP determined in this work (6.73 eV) gives ΔH_f[2-adamantyl cation] = 167 kcal/mol and a hydride affinity of 233.5 kcal/mol.

Strain and Stabilization Energies. The thermodynamic data discussed above and summarized in Table III show that while the

(32) Hargittai, I. *Chem. Commun.* **1971**, 1499.
(33) Engel, P. S.; Chae, W. K.; Baughman, A. S.; Marschke, E. G.; Lewis, E. S.; Timberlake, J. W.; Leudtke, A. E. *J. Am. Chem. Soc.* **1983**, *105*, 5030.
(34) Solomon, J. J.; Field, F. H. *J. Am. Chem. Soc.* **1974**, *97*, 2625.
(35) Gleicher, G. J.; Schleyer, P. v. R. *J. Am. Chem. Soc.* **1967**, *89*, 582.

Table III. Thermochemical Data for the Radicals and Ions[a]

R	$IP_a(R\cdot)$	$\Delta H_f°[R\cdot]$	$\Delta H_f°[R^+]$[d]	$D[R-H]$	$D[R^+-H^-]$[d]
1-adamantyl	(6.21)†	14.8	158.0	98.5	(224.3)[f]
2-adamantyl	(6.73)†	12.3	167.5	(96.0)[c]	233.8
2-methyl-2-butyl	(6.65)†	3.7	156.8	92.6	(228.2)[g]
tert-butyl	(6.70)[b]	(10.3)[c]	164.8	94.8	231.9

[a] All quantities except the IP_a are in kilocalories per mole. The IP_a data are in electron volts. Numbers in parenthesis are either measured or assumed. Numbers with daggers are from this work. The remaining numbers in each row are derived from these values using thermochemical cycles analogous to those shown in Figure 1. Error limits on the derived values are ±1.5 kcal/mol assuming that the assigned values for $\Delta H_f°[(CH_3)_3C\cdot]$ and D[2-adamantyl–H] are correct. Isobutane and isopentane heats of formation are from ref 46; adamantane heat of formation is from the text. [b] Reference 17a. [c] See the Appendix and ref 50. All of the values in this table are referenced to this value for $\Delta H_f°[(CH_3)_3C\cdot]$. [d] See ref 50 for the conventions used in calculating ionic heats of formation and hydride affinities. [e] Assumed value, see text. [f] Derived from the hydride affinity of *tert*-butyl carbonium ion and the relative hydride affinities measured in ref 12. [g] Derived from the relative hydride affinities from ref 34 and the hydride affinity of *tert*-butyl carbonium ion.

1-adamantyl radical is 3.7 ± 1.2 kcal/mol less stable than the *tert*-butyl radical, the 1-adamantyl cation is 7.62 ± 0.1 kcal/mol[12] *more* stable than the *tert*-butyl cation from the differences in bond energies and hydride affinities between adamantane and isobutane. This is surprising since empirical force field (EFF) calculations indicate that II would have a strain energy 12 kcal/mol greater than the strain energy in adamantane,[14] while the corresponding energy difference between the *tert*-butyl cation and isobutane calculated by the same method is only 2.85 kcal/mol.[14] Formation of II has a Δ(strain energy) 9.15 kcal/mol[14] greater than the Δ(strain energy) for formation of the *tert*-butyl cation, yet II is 7.62 kcal/mol more stable[12] than *tert*-butyl cation in the gas phase, implying that II has a total of 16.8 kcal/mol more stabilization than the *tert*-butyl cation. Carbonium ions are known to be more effectively stabilized by hyperconjugative effects than are radicals,[36] and the large stabilization energy in II can be explained on the basis of these effects.[13] Experimental evidence for the presence of C–C hyperconjugation, eq 6, has been found in the

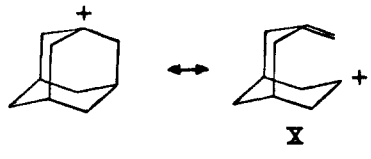

(6)

X

^{1}H NMR spectrum of II in superacid media,[37] which shows the γ protons (δ 5.21) to be more deshileded than the β protons (δ 4.19). In another study, γ-deuterium isotope effects were observed in the solvolysis of 1-adamantyl tosylates and bromides.[13] No β-deuterium isotope effect was observed. Calculations reported with the solvolysis study indicated that the C–C bonds α to the carbocation center shortened by 0.043 Å and β–γ C–C bonds lengthened by 0.050 Å.[13] Such geometry changes could reflect the importance of hyperconjugative resonance forms such as X in stabilizing II. These effects can explain the large stabilization in II since there are three carbons α to the carbocation center with orbitals ideally oriented for homohyperconjugation and C–C hyperconjugation, which are held rigidly in place by the adamantyl cage.

The difference in tertiary C–H bond energies between adamantane and isobutane shows that I is 3.7 ± 1.2 kcal/mol less stable than the *tert*-butyl radical, implying that the Δ(strain energy) for the formation of I is 3.7 kcal/mol greater than the Δ(strain energy) for the formation of *tert*-butyl radical. This result supports the results of studies on the thermal decomposition of azoalkanes,[4] peresters,[5] and other compounds,[6] which suggest the presence of substantial bridgehead strain in I. It does not agree with a more recent study on the thermal decomposition of V, which found no difference between the Δ(strain energy) for the formation of I and the *tert*-butyl radical.[7] Another recent study[8] gave a value of 2.2 kcal/mol for the difference in Δ(strain energy) between I and *tert*-butyl radical, but no error limits were given.

The hydride affinity of the 2-adamantyl cation (233 kcal/mol) shows that it is a highly stabilized carbonium ion compared to typical secondary cations such as isopropyl cation (hydride affinity = 249 kcal/mol) or 2-butyl cation (246 kcal/mol).[18] Hence, the adamantyl cage effectively stabilizes carbonium ions at both possible sites. It is also of interest to note that the norbornyl cation, a secondary C_7 ion, has a hydride affinity of 232 kcal/mol, lower than that of 2-adamantyl cation, a secondary C_{10} species. The low hydride affinity of the 2-norbornyl cation is another example of its unusual stability, which is difficult to explain without invoking nonclassical effects.

In solvolysis the 1- and 2-adamantyl cation systems have been regarded as standards for limiting S_N1 solvolytic behavior. The solvolysis rate of the 1-adamantyl tosylate exceeds that of the 2-isomer by 10^5, corresponding to an energy difference of 7 kcal/mol.[39] The smaller differences in solution than in the gas phase, 9 kcal/mol, suggests a slight preferential solvation of the 2-adamantyl cation relative to the 1-isomer. As discussed elsewhere,[3,39] studies of ion energetics in solution as well as solvolysis studies indicate that the 1-adamantyl cation is itself poorly solvated relative to species such as the *tert*-butyl cation.

Table IV.[a] Determinations of the Heat of Formation of Adamantane

$H_c°(C)$[b]	ΔH_{sub}	$\Delta H_f°(g)$
−1439.89 ± 0.17[c]	14.18 ± 0.04[c]	−32.96 ± 0.19[c]
−1441.95 ± 0.68[d]	14.45 ± 0.30[d]	−30.65 ± 0.98[d]
−1442.01 ± 0.48[e]	14.23 ± 0.20[e]	−30.57 ± 0.90[e]
−1441.01 ± 0.09[f]	14.26 ± 0.20[f]	−32.51 ± 0.32[f]

[a] From Table IV of reference 43. [b] The crystalline heat of combustion. [c] Data from ref 4a. [d] Data from ref 41. [e] Data from ref 42. [f] Data from ref 43. [g] Data from ref 40b.

Conclusion

The geometry changes that occur upon forming four of the possible reactive intermediates, I, II, III, and IV from adamantane have been shown to correlate well with the Franck–Condon envelopes observed in the first bands of the photoelectron spectra for I and III. Thermochemical data related to I, II, III, and IV that agree well with previous experimental and theoretical work have been derived from the adiabatic ionization potentials determined in this work. Unusually large stabilization of the 1- and 2-adamantyl carbonium ions, by mechanisms that have been previously determined,[13] is reflected in the hydride affinities determined in this work and the previous high-pressure mass spectrometry equilibrium measurements.[12] The difference in tertiary C–H bond energies between adamantane and isobutane determined in this work shows that there is more strain energy in I than some recent studies have determined and that alkyl radicals have a stronger preference for planarity than some of these recent studies have suggested.[7,8]

Acknowledgment. We thank J. A. Martinho Simoes and Jocelyn Schultz for helpful conversations.

Appendix

Thermochemistry. In this section the selection of appropriate values for thermochemical data relevant to this study is discussed, along with the errors associated with these data. The heat of formation of adamantane has been obtained by many groups,[40–43]

(36) See ref 14 and references contained therein.
(37) Olah, G. A.; Surya Prakash, G. K.; Shih, J. G.; Krishnamurthy, V. V.; Mateescu, G. D.; Liang, G.; Sipos, G.; Buss, V.; Gund, M. T.; Schleyer, P. v. R. *J. Am. Chem. Soc.* **1985**, *107*, 2764.
(38) Lossing, F. P.; Holmes, J. L. *J. Am. Chem. Soc.* **1984**, *106*, 6917.
(39) Schleyer, P. v. R.; Nicholas, R. D. *J. Am. Chem. Soc.* **1961**, *83*, 2700.
(40) (a) Mansson, M.; Rapport, N.; Westrum, E. F., Jr. *J. Am. Chem. Soc.* **1970**, *92*, 7296. (b) Unpublished results by Dr. M. Mansson. See Table I and ref 12 in: Schulman, J. M.; Disch, R. L. *J. Am. Chem. Soc.* **1984**, *106*, 1202.
(41) Boyd, R. H.; Sanwal, S. N.; Shury-Tehrany, S.; McNally, D. *J. Phys. Chem.* **1971**, *75*, 1264.

and the 1-adamantyl carbonium ion heat of formation has been estimated by several methods.[44,45]

McKervey and Mackle et al.[43] have determined the heats of formation of nine bridged-ring hydrocarbons and critically compared the values they obtained to previous measurements and EFF calculations. The values that they present are summarized in Table IV. From the data in Table IV, it seems most reasonable to choose $\Delta H_f°$[adamantane] = −31.6 ± 0.6 kcal/mol.

Of the published values for $\Delta H_f°$[II], one[44] requires the estimation of $\Delta H_f°$[1-adamantyl bromide] and another[45] requires the estimation of both $\Delta H_f°$[1-adamantyl bromide] and $\Delta H_f°$[1-adamantyl chloride] by group methods. Benson's group method fails for adamantane, giving $\Delta H_f°$[adamantane] = −36.52 kcal/mol.[46] This is not surprising since a substantial amount of strain energy in the adamantane ring system is predicted by EFF calculations.[14] On this basis, there is no reason to expect that the group method can be applied successfully to calculations of the heats of formation of 1-chloro- and 1-bromo-adamantane. Hence, estimates of $\Delta H_f°$[II] calculated from estimated heats of formation of the 1-halo-adamantanes must be regarded with suspicion.

A reliable estimate of $\Delta H_f°$[II] can be derived from a photoionization appearance potential measurement of II from adamantane.[47] The appearance potential obtained, 10.6 eV, yields $\Delta H_f°$[II] = 160 kcal/mol. This value should be a good estimate since 1,2-hydride shifts are not allowed in II,[48] and Schwarz[49] has shown that loss of hydrogen occurs exclusively at the bridgehead sites in electron impact ionization of adamantane, so that II should be the only ion formed by the loss of hydrogen from the parent adamantyl radical ion. Comparison of this absolute value for $\Delta H_f°$[II] to the values for the relative hydride affinity of II from the gas-phase equilibrium studies presented in Table X is made difficult by uncertainty in the value for $\Delta H_f°[(CH_3)_3C\cdot]$,[50] which leads to uncertainty in the value for $\Delta H_f°[(CH_3)_3C^+]$. Choosing $\Delta H_f°[(CH_3)_3C\cdot]$ = 10.3 ± kcal/mol gives $\Delta H_f°[(CH_3)_3C^+]$ = 165 kcal/mol.[51] Then, from Kebarle and Sharma's measurement of ΔH for reaction 1, with $\Delta H_f°$[adamantane] and $\Delta H_f°$[isobutane], $\Delta H_f°$[II] is calculated to be 158 ± 3 kcal/mol, in good agreement with the value calculated from the ionization potential measurement mentioned above.

Clearly, the measurement of $\Delta H°$ for reaction 1 by high-pressure mass spectrometry equilibrium experiments is the most precise, and it is this value that was used to calculate the difference in tertiary bond energies between adamantane and isobutane. It should be stressed that this difference is known to a precision of ±1 kcal/mol, but the final assignment of absolute bond energies must await agreement on a value for $\Delta H_f°[(CH_3)_3C\cdot]$.

(42) Butler, R. S.; Carson, A. S.; Laye, P. G.; Steele, W. V. *J. Chem. Thermodyn.* **1971**, *3*, 277.
(43) Clark, T.; Mc O. Knox, T.; McKervey, M. A.; Mackle, H.; Rooney, J. J. *J. Am. Chem. Soc.* **1979**, *101*, 2404.
(44) Fort, R. C. In *Carbonium Ions*; Olah, G. A., Schleyer, P. v. R., Eds.; Wiley: New York, 1973; Vol. IV, p 1783 ff.
(45) Allison, J.; Ridge, D. P. *J. Am. Chem. Soc.* **1979**, *101*, 4998.
(46) Group values from: Cox, S. C.; Pilcher, G. *Thermochemistry of Organic and Organometallic Compounds*; Academic: New York, 1970.
(47) Federova, M. S.; Potapov, V. K.; Denisor, Yu. V.; Sorokin, v. V.; Erlasheva, T. I. *Zh. Fiz. Khim.* **1974**, *48*, 1828; *Russ. J. Phys. Chem. Engl. Transl.* **1974**, *48*, 1078.
(48) Schleyer, P. v. R.; Lam, L. K. M.; Raber, D. F.; Fry, J.L.; McKervey, M. A.; Alford, J. R.; Cuddy, B. D.; Keizer, V. G.; Celuk, H. W.; Schlatmann, J. L. M. A. *J. Am. Chem. Soc.* **1970**, *92*, 5246.
(49) Wesdemiotis, C.; Schilling, M.; Schwarz, H. *Angew. Chem., Int. Ed. Engl.* 1979, *18*, 950; *Angew. Chem.* **1979**, *91*, 1017.
(50) (a) Doering, W. v. E. *Proc. Natl. Acad. Sci. U.S.A.* **1981**, *78*, 5279. $\Delta H_f[(CH_3)_3^+]$ = 165 kcal/mol was calculated from $\Delta H_f[(CH_3)_3\cdot]$ = 10.3 kcal/mol from ref 50a and the IP_a of $(CH_3)_3\cdot$ from ref 17a. The ionic heat of formation was calculated by using the convention that the heat of formation of an electron at rest is zero at all temperatures.[51] Therefore, $\Delta H_f[H^-]$ = 34.7 kcal/mol.[51] Some recent results that support a high value for $\Delta H_f[(CH_3)_3C\cdot]$ were reported by Tsang (ref 50b), who obtained $\Delta H_f[(CH_3)_3C\cdot]$ = 12.3 kcal/mol. (b) Tsang, W. *J. Am. Chem. Soc.* **1985**, *107*, 2872.
(51) Rosenstock, H. M; Draxl, K.; Steiner, B. W.; Herron, J. T. *J. Phys. Chem. Ref. Data, Suppl.* **1977**, 6.

Structures and Energies of Singlet Silacyclopropenylidene and 14 Higher Lying C_2SiH_2 Isomers

Gernot Frenking, Richard B. Remington, and Henry F. Schaefer III*

Contribution from the Department of Chemistry, University of California, Berkeley, California 94720. *Received December 21, 1984*

Abstract: The closed-shell molecular structures and relative energies of 15 different isomers of the formula C_2SiH_2 have been investigated via nonempirical molecular electronic structure theory. Eight structures were found to be minima on the self-consistent-field potential energy hypersurface by using a double-ζ (DZ) basis set. The three lowest lying isomers have further been optimized with the DZ basis set augmented by polarization functions (DZ+P), and vibrational frequencies and IR intensities were obtained at this level of theory by using analytical gradients and second derivatives. Correlation energies have been predicted at the DZ+P level via configuration interaction including all single and double excitations of the valence orbitals (DZ+P CI). 3-Silacyclopropenylidene (**1**) has clearly been found to be the global minimum on the singlet C_2SiH_2 potential energy hypersurface. Vinylidenesilene (**2**) and silylenylacetylene (**3**) are 17 and 22 kcal/mol higher in energy, respectively (DZ+P CI). While **1**, **2**, and **3** might experimentally be observed, the other isomers are higher in energy, and it is less likely that they will soon be identified.

Theoretical[1] and experimental[2] studies of triatomic SiC_2 structures have shown perhaps surprisingly that the cyclic singlet isomer with a CC triple bond is the global minimum of the SiC_2 potential energy hypersurface. By comparison, the C_3 molecule has a linar $^1\Sigma_g^+$ ground state.[3] In addition the related Si_2C molecule has recently been predicted to have a nonlinear energy minimum.[4] Thus, the substitution of carbon by silicon may result in very different structures for the lowest lying isomers of simple

(1) Grev, R. S.; Schaefer, H. F., III *J. Chem. Phys.* **1984**, *80*, 3552.
(2) Michalopoulos, D. L.; Geusic, M. E.; Langridge-Smith, P. R. R.; Smalley, R. E.; *J. Chem. Phys.* **1984**, *80*, 3556.
(3) Douglas, A. E. *Astrophys. J.* **1951**, *114*, 466. Gausset, L.; Herzberg, G.; Lagerqvist, A.; Rosen, A. *Ibid.* **1965**, *142*, 45. Liskow, D. H.; Bender, C. F.; Schaefer, H. F. *J. Chem. Phys.* **1972**, *56*, 5075. Whiteside, R. A.; Krishnan, R.; Frisch, M. J.; Pople, J. A.; Schleyer, P. v. R. *Chem. Phys. Lett.* **1981**, *80*, 547.
(4) Grev, R. S.; Schaefer, H. F. *J. Chem. Phys.*; in press.

0002-7863/86/1508-2169$01.50/0